BALLISTIC LIMIT OF THIN CFRP PLATES

HIGASHIDE Masumi[(1)], NAGAO Yosuke[(1)], KIBE Seishiro[(1)], Alessandro Francesconi[(2)] , Daniele Pavarin[(2)]

[(1)]Japan Aerospace Exploration Agency, 6-13-1, Ohsawa, Mitaka, Tokyo 101-0015, JAPAN,
Email: higaside@chofu.jaxa.jp, nagao@chofu.jaxa.jp, kibe.seishiro@jaxa.jp
[(2)]CISAS University of Padova, Via Venezia 15, 35131 Padova, ITALY,
Email: alessandro.francesconi@unipd.it, daniele.pavarin@unipd.it

ABSTRACT

JAXA (Japan Aerospace Exploration Agency) has carried out the hypervelocity impact tests for carbon fiber reinforced plastic (CFRP) plates together with CISAS (Centre of Studies and Activities for Space), University of Padova. Quasi-isotropic CFRP plates of 2.3, 3.5, and 4.7 mm in thickness were tested. Aluminum sphere of 0.8 to 2.9 mm in diameter was used as a projectile. The projectile was launched in a velocity range of 2 to 5 km/sec. The projectile impacted on the target in the normal direction. After the impact, peeling along the fiber direction was observed on the surface of the target. Moreover, delamination was generated near the surface of the target. A ballistic limit equation for CFRP was calculated by modifying the Cour-Palais equation. The ballistic limit equation for CFRP showed the good agreement with the test results.

1. INTRODUCTION

Carbon fiber reinforced plastic (CFRP) is applied to many parts of a spacecraft since it is low weight and high strength. In a spacecraft, CFRP is frequently employed as material of large and exposed parts, for example, structures, solar arrays, and antennas. Therefore, CFRP has a high probability of impacts of space debris. CFRP is often used as material of face sheets of a honeycomb sandwich panel. Thus hypervelocity impact tests for honeycomb sandwich structure have already been performed [1-3]. However, hypervelocity impact phenomena of a CFRP plate without a honeycomb core have not been studied enough. Since material properties of CFRP are improved day by day, it is expected that CFRP is employed as material of a spacecraft more and more. On the other hand, debris environment will become worse. Therefore, it is necessary to know damage of CFRP caused by debris impact.

The purpose of this study is to investigate damage of CFRP caused by hypervelocity impacts and to know a ballistic limit of a CFRP plate. JAXA has carried out hypervelocity impact tests for CFRP plates together with CISAS since 2003 [4,5]. CISAS has performed the hypervelocity impact tests with a two-stage light gas gun. After the impact tests, JAXA has performed non-destructive inspection of the targets.

2. HYPERVELOCITY IMPACT TESTS

The CFPR plates used in this study are shown in Tab. 1. IM600/133 is made of high strength carbon fibers and high toughness epoxy. The hypervelocity impact tests have been performed with a two-stage light gas gun of CISAS [6,7]. Aluminum spheres of 0.8 to 2.8 mm in diameter were employed as projectiles. The projectiles were launched in a velocity range of 2 to 5 km/sec. The projectile impacted on the target in the normal direction. After the impacts, a perforation hole or a crater of the target is sometimes filled with chopped and shattered carbon fibers. Therefore, in some cases, the perforation hole looks like the crater. It is difficult to judge the perforation by observation of the hole. In order to know whether the projectile perforated the target or not, a copper plate was installed behind the target as a witness plate as shown in Fig. 1. The perforation of the projectile was confirmed by aluminum craters generated by fragments of the projectile on the witness plate.

Table 1 Targets

Prepreg	Unidirectional IM600/133, (TOHO TENAX)
Stacking	Quasi-isotropic Lamination 16ply, 24ply, 32ply
Thickness	2.2mm, 3.3mm, 4.5mm

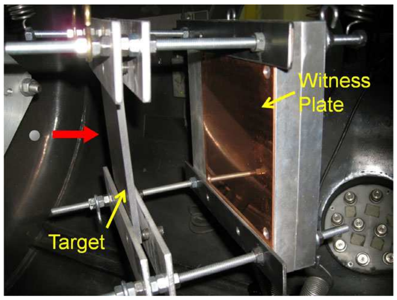

Figure 1 Target and Witness Plate

Proc. '5th European Conference on Space Debris', Darmstadt, Germany
30 March – 2 April 2009, (ESA SP-672, July 2009)

The test results are shown in Tabs. 2-4. In total, 37 perforation data and 17 non-perforation data were obtained. The perforated targets are shown in Figs. 2-4. Peelings along the fiber direction were observed on the surfaces of both the front and the back. When the perforation hole was found clearly as shown in Figs. 2-3, some fibers protruded from interlamination. As shown in Fig. 4, the perforation hole looked like the crater in some cases since the hole was filled with the chopped and shattered fibers. The non-perforated targets are shown in Figs. 5-7. On the front surface of the targets, peelings along the fiber direction were found like the perforation results. When the impact energy was larger, peelings along the fiber direction were also observed on the back surfaces as shown in Fig. 6. Moreover, the part under the craters was fractured hard. In the case of smaller impact energy, peelings were not generated on the back surfaces but some cracks were produced as shown in Figs. 5 and 7. All the cracks on the back surface were generated along the fiber direction. It is considered that the peelings and the cracks occurred due to the impact pressure reaching to the target surface. The lamination of the surfaces was damaged by the tensile stress caused by the impact pressure reaching to the target surface. CFRP has high strength in the direction of the fibers but the strength in the normal direction of the fibers is extremely low. Therefore, the peeling and the cracks were produced along the fiber direction.

Table 2 Test Results, 16ply (t=2.2mm)

Shot ID	Impact Velocity, V_p [km/sec]	Projectile Diameter, d_p [mm]	Result
6392	4.96	1.5	Perforation
6493	4.09	1.5	Perforation
6496	3.79	2.3	Non-Perforation
6507	1.93	0.8	Perforation
6513	2.05	1.5	Perforation
6516	2.06	2.3	Perforation
6576	5.01	2.3	Perforation
6588	4.56	0.8	Perforation
6616	3.83	0.8	Perforation
7216	4.01	2.9	Perforation
7234	2.12	2.9	Perforation
7240	2.13	1.9	Perforation
7254	4.31	1.9	Perforation
7515	4.58	2.9	Perforation
8349	3.17	0.8	Non-Perforation
8350	3.15	0.8	Non-Perforation
8354	2.38	0.8	Non-Perforation
8355	2.38	0.8	Non-Perforation

Table 3 Test Results, 24ply (t=3.3mm)

Shot ID	Impact Velocity, V_p [km/sec]	Projectile Diameter, d_p [mm]	Result
6487	3.97	0.8	Non-Perforation
6490	4.19	1.5	Perforation
6495	3.67	2.3	Perforation
6505	1.96	0.8	Non-Perforation
6510	1.99	1.5	Non-Perforation
6515	1.81	2.3	Perforation
6575	5.00	2.3	Perforation
6587	4.83	0.8	Perforation
6658	4.98	1.5	Perforation
7203	4.90	1.9	Perforation
7215	4.00	2.9	Perforation
7233	2.29	2.9	Perforation
7253	3.63	1.9	Perforation
7514	4.69	2.9	Perforation
8339	3.19	1.5	Perforation
8343	2.34	1.5	Non-Perforation
8352	3.79	0.8	Non-Perforation
8360	4.93	0.8	Non-Perforation

Table 4 Test Results, 32ply (t=4.5mm)

Shot ID	Impact Velocity, V_p [km/sec]	Projectile Diameter, d_p [mm]	Result
6385	5.02	1.5	Perforation
6486	3.81	0.8	Non-Perforation
6489	4.07	1.5	Perforation
6494	4.07	2.3	Perforation
6502	1.98	0.8	Non-Perforation
6509	2.09	1.5	Non-Perforation
6514	2.03	2.3	Perforation
6574	5.02	2.3	Perforation
6581	5.17	0.8	Non-Perforation
7202	5.09	1.9	Perforation
7214	3.88	2.9	Perforation
7217	4.18	1.9	Perforation
7223	2.19	2.9	Perforation
7235	2.41	1.9	Non-Perforation
7513	4.85	2.9	Perforation
8336	3.92	1.5	Perforation
8337	3.19	1.5	Perforation
8342	2.29	1.5	Non-Perforation

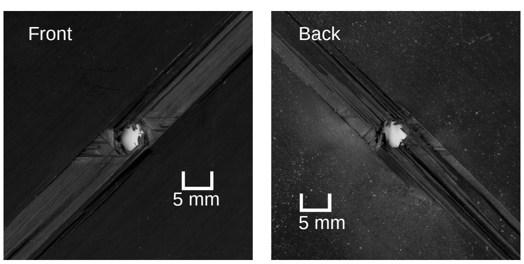

Figure 2 Perforation, 16ply (t=2.2mm), V_p=5.01km/sec, d_p=2.3mm

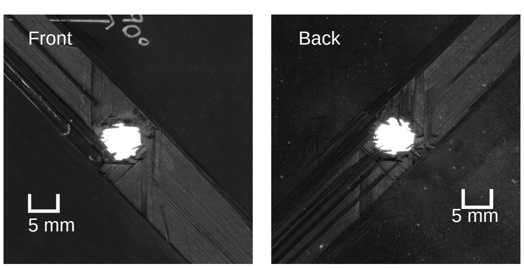

Figure 3 Perforation, 24ply (t=3.3mm), V_p=4.69km/sec, d_p=2.9mm

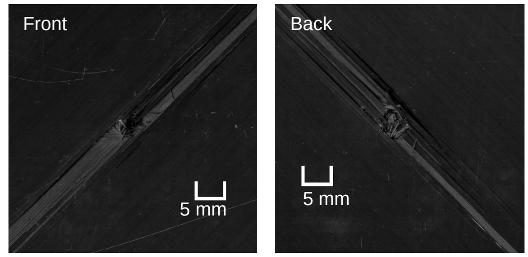

Figure 4 Perforation, 32ply (t=4.5mm), V_p=4.07km/sec, d_p=1.5mm

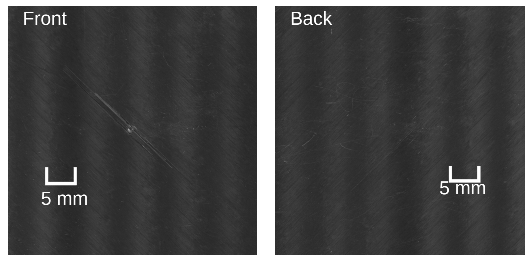

Figure 5 Non-perforation, 16ply (t=2.2mm), V_p=2.38km/sec, d_p=0.8mm

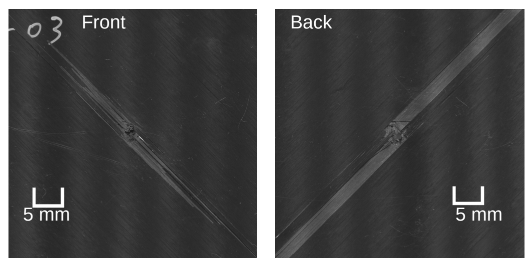

Figure 6 Non-perforation, 24ply (t=3.3mm), V_p=2.34km/sec, d_p=1.5mm

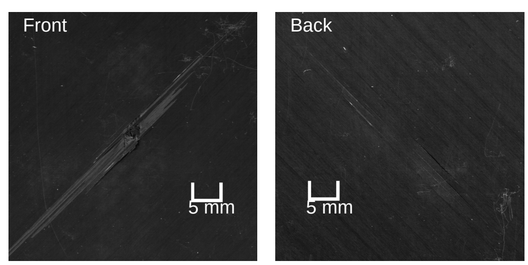

Figure 7 Non-perforation, 32ply (t=4.5mm), V_p=2.09km/sec, d_p=1.5mm

3. NON-DESTRUCTIVE INSPECTION

In JAXA, delamination generated by the impact on the CFRP plate was observed with ultrasonic testing using a single probe. Results of the perforated targets are shown in Figs. 8-10 and results of the non-perforated targets are shown in Figs. 11-13. Colour of the image showing the result of ultrasonic testing does not mean damage level. The colour expresses only the place of the delamination. It is found that the delamination area is larger than the cross section of the perforation hole or the crater. All of the delamination was generated at the place of approximately 1 mm from the target surface. Even when the peeling of the back surface of the target was not produced, the delamination of the back surface was observed as shown in Figs. 5 and 7. The stress needed to generate the delamination depends on strength of the epoxy. Therefore, the delamination can occur by lower impact pressure than the peeling. Consequently, the delamination was produced even though the peeling was not observed. The relationship between the delamination area of the targets and the impact energy of the projectile is shown in Fig. 14. The delamination area increased with the impact energy. Compared with the trends of perforation data, the trend of non-perforation data was sharper rise. In order to explain the delamination and the peeling phenomena, authors will do the numerical simulation of hypervelocity impact on CFRP plates.

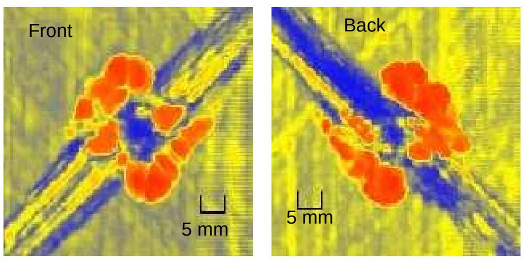

Figure 8 Ultrasonic Testing, Perforation, 16ply (t=2.2mm), V_p=5.01km/sec, d_p=2.3mm

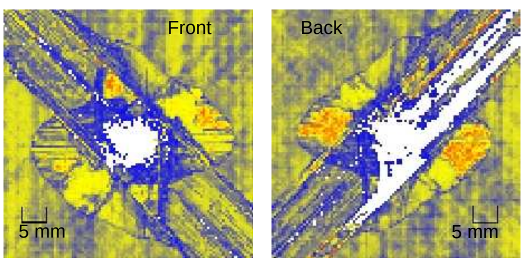

Figure 9 Ultrasonic Testing, Perforation, 24ply (t=3.3mm), V_p=4.69km/sec, d_p=2.9mm

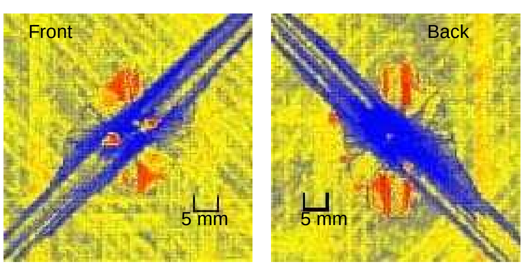

Figure 10 Ultrasonic Testing, Perforation, 32ply (t=4.5mm), V_p=4.07km/sec, d_p=1.5mm

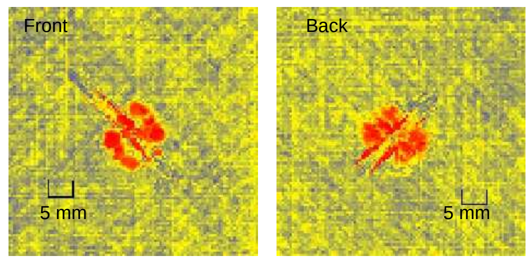

Figure 11 Ultrasonic Testing, Non-perforation, 16ply (t=2.2mm), V_p=2.38km/sec, d_p=0.8mm

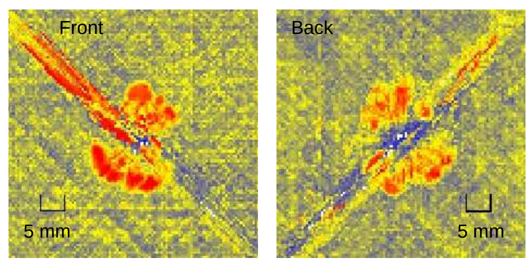

Figure 12 Ultrasonic Testing, Non-perforation, 24ply (t=3.3mm), V_p=2.34km/sec, d_p=1.5mm

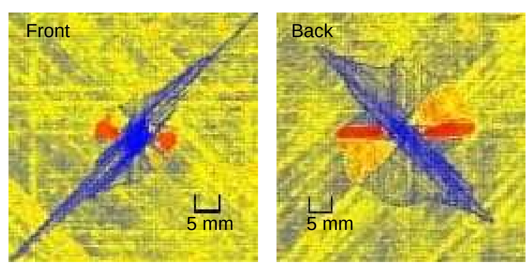

Figure 13 Ultrasonic Testing, Non-perforation, 32ply (t=4.5mm), V_p=2.09km/sec, d_p=1.5mm

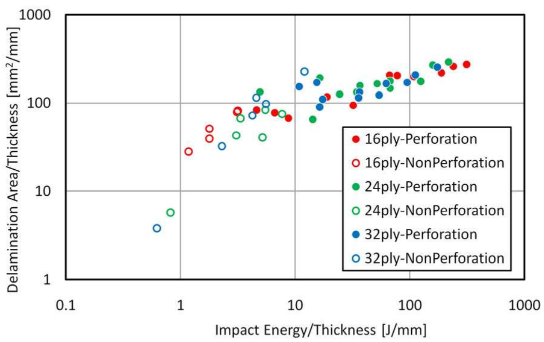

Figure 14 Relationship between Impact Energy and Delamination Area

4. BALLISTIC LIMIT EQUATION

In this study, a ballistic limit equation for a CFRP plate was calculated by modifying the ballistic limit equation reported by B.G. Cour-Palais [8,9]. The Cour-Palais ballistic limit equation has been based on depth of a crater generating on a semi-infinite plate by an impact of a projectile. The depth of a crater, P (cm) is calculated by the following equations.

For $\rho_p/\rho_t < 1.5$,

$$P = 5.24\, d_p^{\frac{19}{18}} H^{-\frac{1}{4}} \left(\frac{\rho_p}{\rho_t}\right)^{\frac{1}{2}} \left(\frac{V_n}{C_n}\right)^{\frac{2}{3}} \qquad (1)$$

For $\rho_p/\rho_t \geq 1.5$,

$$P = 5.24\, d_p^{\frac{19}{18}} H^{-\frac{1}{4}} \left(\frac{\rho_p}{\rho_t}\right)^{\frac{2}{3}} \left(\frac{V_n}{C_n}\right)^{\frac{2}{3}} \qquad (2)$$

where d_p (cm) is diameter of a projectile, H is Brinell hardness of a target, ρ_t (g/cm^3) is density of a target, ρ_p (g/cm^3) is density of the projectile, V_n (km/sec) is normal component of impact velocity to a target surface, and C_n (km/sec) is normal component of sound speed of a target in the direction of the thickness. When a projectile perforates a target, the relationship between P and target thickness causing perforation of a projectile, t_c is given as the following.

$$t_c = 1.8P \qquad (3)$$

By using Eqs. 1-3, the Cour-Palais ballistic limit equations are calculated as following equations.

For $\rho_p/\rho_t < 1.5$,

$$d_c = \left\{ 0.11 t\, H^{\frac{1}{4}} \left(\frac{\rho_p}{\rho_t}\right)^{-\frac{1}{2}} \left(\frac{V_n}{C_n}\right)^{-\frac{2}{3}} \right\}^{\frac{18}{19}} \qquad (4)$$

For $\rho_p/\rho_t \geq 1.5$,

$$d_c = \left\{ 0.11 t\, H^{\frac{1}{4}} \left(\frac{\rho_p}{\rho_t}\right)^{-\frac{2}{3}} \left(\frac{V_n}{C_n}\right)^{-\frac{2}{3}} \right\}^{\frac{18}{19}} \qquad (5)$$

where d_c (cm) is critical diameter of a projectile causing perforation, t (cm) is target thickness.

In order to apply above procedure to calculation of a ballistic limit equation for a CFRP plate, it is necessary to investigate a depth of crater generated by an impact on a CFRP plate. However, it is difficult to measure a depth of a crater on the CFRP plate since the crater is filled with chopped or shattered carbon fibers. Consequently, the ballistic limit equation for a CFRP plate was calculated by regression of the test data to the Cour-Palais ballistic limit equation.

In this study, the projectiles were made of aluminum (ρ_p = 2.7 g/cm^3) and the targets were made of CFRP (ρ_t = 1.5 g/cm^3). Since ρ_p/ρ_t = 1.8, Eq. 5 was modified to express the ballistic limit of a CFRP plate. The target material was the same in all tests. Therefore, H and ρ_p/ρ_t were constant. By using constant, α, the ballistic limit of a CFRP plate is assumed as the following equation.

$$d_c = \left\{ \alpha \times t \left(\frac{V_p}{C_n}\right)^{-\frac{2}{3}} \right\}^{\frac{18}{19}} \qquad (6)$$

where V_n of Eq. 5 is replaced with V_p since only normal impacts are considered in this study. With least square method, α is calculated from the test data. As a result, the following equation was obtained.

$$d_c = \left\{ 0.39 \times t \left(\frac{V_p}{C_n}\right)^{-\frac{2}{3}} \right\}^{\frac{18}{19}} \qquad (7)$$

Additionally, in order to express the ballistic equation simply, it is assumed that 18/19 of Eq. 6 is approximately 1. By using constant, β, Eq. 6 is rewritten in the following equation.

$$d_c = \beta \times t \left(\frac{V_p}{C_n}\right)^{-\frac{2}{3}} \qquad (8)$$

β is calculated from the test data by least square method and the following equation was obtained.

$$d_c = 0.38 \times t \left(\frac{V_p}{C_n}\right)^{-\frac{2}{3}} \qquad (9)$$

The test results were compared with the ballistic limit equations calculated from Eqs. 7 and 9, as shown in

Figs. 15-17. The closed and opened circles investigate the results of perforation and non-perforation, respectively. The ballistic limit equations showed the good agreement with the test results. As shown in Figs. 15-17, Eqs. 7 and 9 showed almost the same results. Consequently, it was found that Eq. 9 is useful as the ballistic limit equation for CFRP plates as well as Eq. 7.

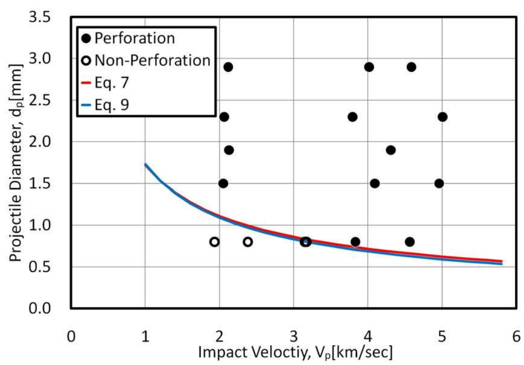

Figure 15 Ballistic Limit of CFRP Plate, 16ply (t=2.2mm)

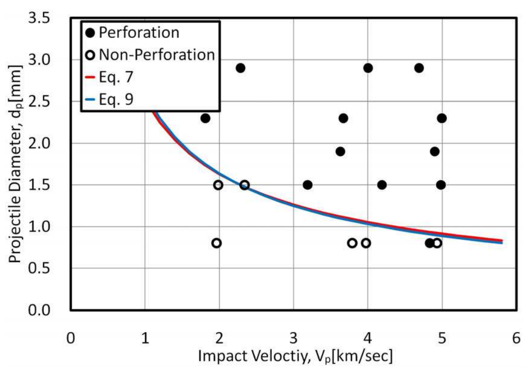

Figure 16 Ballistic Limit of CFRP Plate, 24ply (t=3.3mm)

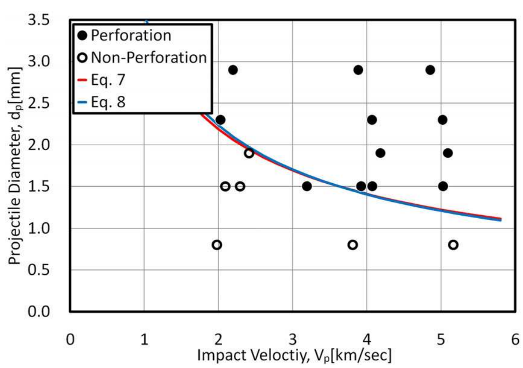

Figure 17 Ballistic Limit of CFRP Plate, 32ply (t=4.5mm)

5. SUMMARY

JAXA has carried out the hypervelocity impact tests for CFRP plates together with CISAS. Quasi-isotropic CFRP plates of 2.3, 3.5, and 4.7 mm in thickness were tested. CISAS performed the hypervelocity impact tests. Aluminum spheres of 0.8 to 2.8 mm in diameter were launched in a velocity range of 2 to 5 km/sec. JAXA performed non-destructive inspection of the targets, after the impact tests. Moreover, a ballistic limit equation for CFRP was calculated by modifying the Cour-Palais equation. The following results were obtained.

- On the surfaces of the CFRP plate, the peelings or the cracks along the fiber direction were observed.
- The crater and the perforation hole were filled with chopped and shattered fibers.
- The delamination area of the CFRP plate was larger than the cross section of the perforation hole or the crater.
- The delamination was generated near the surface of the CFRP plate.
- The ballistic limit equation for CFRP plates showed the good accordance with the test results.

In this study, the ballistic limit equation for CFRP plates was obtained. However, the equation is applicable to only normal impacts. In order to modify this equation, oblique impact tests will be performed. Additionally, numerical simulation of hypervelocity impact on CFRP plates should be done for understanding of the delamination and the peeling phenomena.

REFERENCES

1. Taylor, E.A., Herbert, M.K., Vaughan, B.A.M. & Mcdonnell, J.A.M. (1999). Hypervelocity Impact on Carbon Fibre Reinforced Plastic / Aluminum Honeycomb: Comparison with Whipple Bumper Shields. *Int. J. Impact Eng*. **23**, 883-893.
2. Sibeaud, J.M., Prieur, C. & Puillet, C. (2005). Hypervelocity Impact on Honeycomb Target Structures: Experimental Part. In *Proc.4th European Conference on Space Debris* (Ed. D. Danesy), ESA SP-587, ESA Publications Division. European Space Agency, Noordwijk, The Netherlands, pp401-405.
3. Ryan, S., Wicklein, M., Mouritz, A., Riedel, W., Schäfer, F. & Thoma, K. (2009). Theoretical Prediction of Dynamic Composite Material Properties for Hypervelocity Impact Simulations. *Int. J. Impact Eng*. **36**, 899-912.

4. Daigo, K., Nagao, Y., Kibe, S. & Francesconi, A. (2004). Hypervelocity Impact Studies on Composite Material, In *Proc.55th IAC*. International Astronautical Federation, Paris, France.
5. Nagao, Y., Kibe, S., Daigo, K., Francesconi, A. & Pavarin, D. (2005). Hyper Velocity impact Studies Simulating Debris Collision on Composites Material. In *Proc.4th European Conference on Space Debris* (Ed. D. Danesy), ESA SP-587, ESA Publications Division. European Space Agency, Noordwijk, The Netherlands, pp413-418.
6. Pavarin, D., Francesconi, A., Niero, F. & Angrilli, F. (2006). Active Piston Technique to Optimize the Chamber Pressure in Two-Stage Light-Gas Guns. *Int. J. Impact Eng*. **33**, 562-604.
7. Pavarin, D. & Francesconi, A. (2003). Improvement of the CISAS High-Shot-Frequency Light-Gas Gun. *Int. J. Impact Eng*. **29**, 549-562.
8. Cour-Palais, B.G. (1985). Hypervelocity Impact Investigations and Meteoroid Shielding Experience Related to Apollo and Skylab. In *Proc. Space Debris Workshop* (Eds. D.J. Kessler & S.Y. Su), NASA CP 2360, NASA Scientific and Technical Information Branch. National Aeronautics and Space Administration, Hampton, US, pp247-275.
9. Cour-Palais, B.G. (1987). Hypervelocity Impact in Metals, Glass and Composites. *Int. J. Impact Eng*. **5**, 221-237.